International Journal of Thermophysics, Vol. 13, No. 1, 1992

Error Analysis by Numerical Simulation for a Three-Color Pyrometer Assuming a Blackbody Spectrum and a Wavelength- and Temperature-Dependent Emissivity[1]

G. R. Gathers[2]

A numerical method devised to test ratio pyrometers has been used to explore the fitting of a blackbody spectrum and an emissivity model that assumes linear wavelength dependence and arbitrary temperature dependence. The slope and intercept coefficients for the emissivity and the temperature form three unknowns. The equations for the output of the three channels can be solved simultaneously for the emissivity coefficients and the temperature at any given time using the corresponding measured channel outputs. The stability of the solution is tested as a function of the temperature and equipment characteristics.

KEY WORDS: high temperatures; multiwavelength pyrometer; pyrometry; temperature measurements.

1. INTRODUCTION

The preceding paper [1] describes a system for numerically evaluating the measurement errors for a ratio pyrometer assuming constant emissivity. A linear ramp of temperature versus time is assumed and artificial data are generated. These artificial data are then modulated by square waves of constant amplitude. The altered artificial data are then processed by the data reduction scheme to observe the resulting temperature excursions caused by the modulation. Quantitative bounds on the temperature can be determined corresponding to a given precision in the input data. The modulation method can also be used to evaluate the behavior of a pyrometer scheme with a given choice of hardware.

[1] Paper presented at the Second Workshop on Subsecond Thermophysics, September 20–21, 1990, Torino, Italy.

[2] Lawrence Livermore National Laboratory, University of California, Livermore, California 94550, U.S.A.

0195-928X/92/0100-0187$06.50/0

2. METHOD

We consider a scheme in which the emissivity is assumed to have linear dependence on wavelength and arbitrary dependence on temperature:

$$\varepsilon(\lambda, T) = a_0(T) + a_1(T)\,\lambda \tag{1}$$

The response of a given channel is given by

$$R_i(T) = G \int_0^\infty D_i(\lambda)\, B_i(\lambda)\, W(\lambda, T)\, \varepsilon(\lambda, T)\, d\lambda \tag{2}$$

where $D_i(\lambda)$ and $B_i(\lambda)$ describe the spectral response of the detector and optical elements, respectively, $W(\lambda, T)$ is the blackbody spectral density, and ε is the emissivity. G includes factors such as solid angle attenuation which are assumed to be the same for all channels. Substituting Eq. (1) in Eq. (2) gives

$$R_i(T) = Ga_0(T) \int_0^\infty D_i(\lambda)\, B_i(\lambda)\, W(\lambda, T)\, d\lambda + Ga_1(T) \int_0^\infty D_i(\lambda)\, B_i(\lambda)\, W(\lambda, T)\, \lambda\, d\lambda \tag{3}$$

Define

$$F_i(T) = \int_0^\infty D_i(\lambda)\, B_i(\lambda)\, W(\lambda, T)\, d\lambda \tag{4}$$

and

$$H_i(T) = \int_0^\infty D_i(\lambda)\, B_i(\lambda)\, W(\lambda, T)\, \lambda\, d\lambda \tag{5}$$

so that

$$R_i(T) = Ga_0(T)\, F_i(T) + Ga_1(T)\, H_i(T) \tag{6}$$

For three channels, we may write

$$R_1^* = Ga_0(T)\, F_1(T) + Ga_1(T)\, H_1(T) \tag{7}$$

$$R_2^* = Ga_0(T)\, F_2(T) + Ga_1(T)\, H_2(T) \tag{8}$$

$$R_3^* = Ga_0(T)\, F_3(T) + Ga_1(T)\, H_3(T) \tag{9}$$

where the asterisk denotes experimental values. Eliminating a_0 and a_1 between the three equations gives

$$R_1^*\omega_1(T) + R_2^*\omega_2(T) + R_3^*\omega_3(T) = 0 \tag{10}$$

where

$$\omega_1 = H_2F_3 - H_3F_2 \tag{11}$$

$$\omega_2 = H_3F_1 - H_1F_3 \tag{12}$$

$$\omega_3 = H_1F_2 - H_2F_1 \tag{13}$$

and we have divided out the factor G. Tables of $F_i(T)$, $H_i(T)$, and $\omega_i(T)$ may be calculated for the chosen hardware. Root finding methods may then be used to solve Eq. (10) for T. We then have

$$a_0(T) = \frac{R_2^*H_1(T) - R_1^*H_2(T)}{\omega_3(T)} \tag{14}$$

and

$$a_1(T) = \frac{R_1^* - a_0(T)\,F_1(T)}{H_1(T)} \tag{15}$$

Equations (7)–(9) thus form three equations in three unknowns, T, a_0, and a_1, which are solved simultaneously to give a unique solution. Note that the measured detector responses need not be absolute measurements, so no calibrating lamp is needed. We will determine the sensitivity of the solution to the precision of the measurements R_1^*, R_2^*, and R_3^*, and channel placement and bandwidth.

3. RESULTS

Three initial problems were considered to examine the influence of channel width and the wavelength separation between channels. Errors of 0.2% and Gaussian channels were used in each case.

For problem 1, the channels has 50-nm full width at half-maximum (FWHM), and the wavelengths were 500, 700, and 900 nm. Problem 2 used 50-nm FWHM and wavelengths 550, 650, and 700 nm. Problem 3 used 100-nm FWHM and wavelengths 550, 650, and 700 nm.

Figures 1, 2, and 3 show the results for these problems. Comparison of Figs. 1 and 2 shows that there is significant dependence on the wavelength separation of the channels. The best results are obtained for

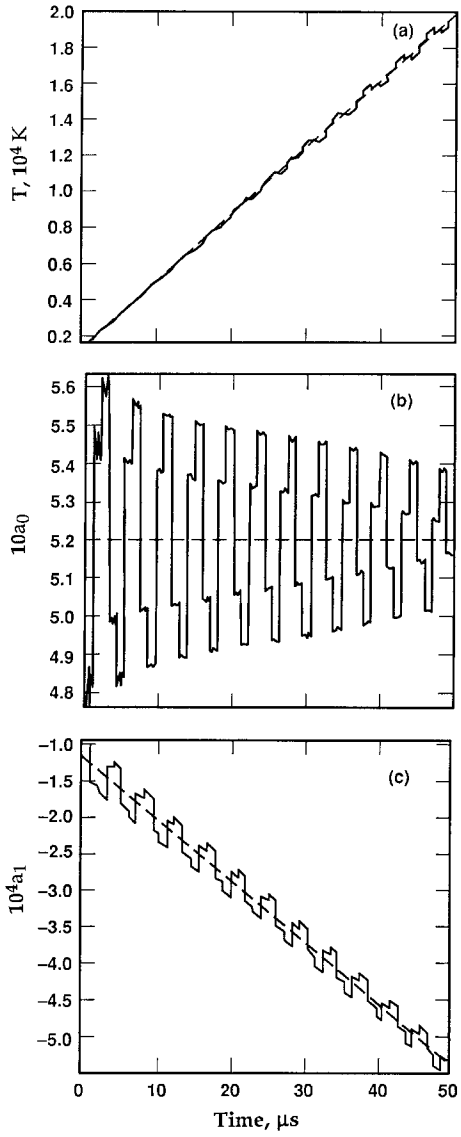

Fig. 1. Measurement errors for T, a_0, and a_1 for problem 1, with Gaussian channels with 50-nm FWHM, 0.2% errors, and wavelengths 500, 700, and 900 nm.

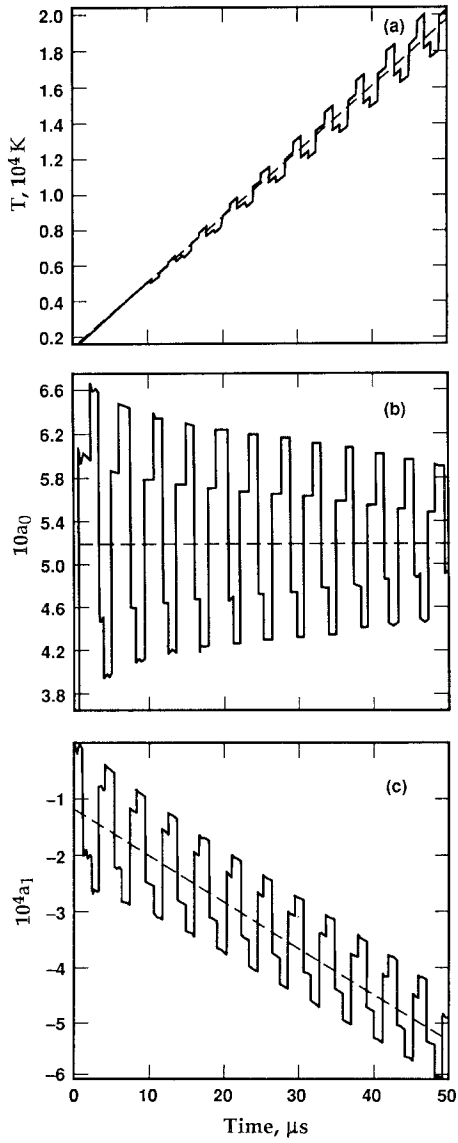

Fig. 2. Measurement errors for T, a_0, and a_1 for problem 2, with Gaussian channels with 50-nm FWHM, 0.2% errors, and wavelengths 550, 650, and 750 nm.

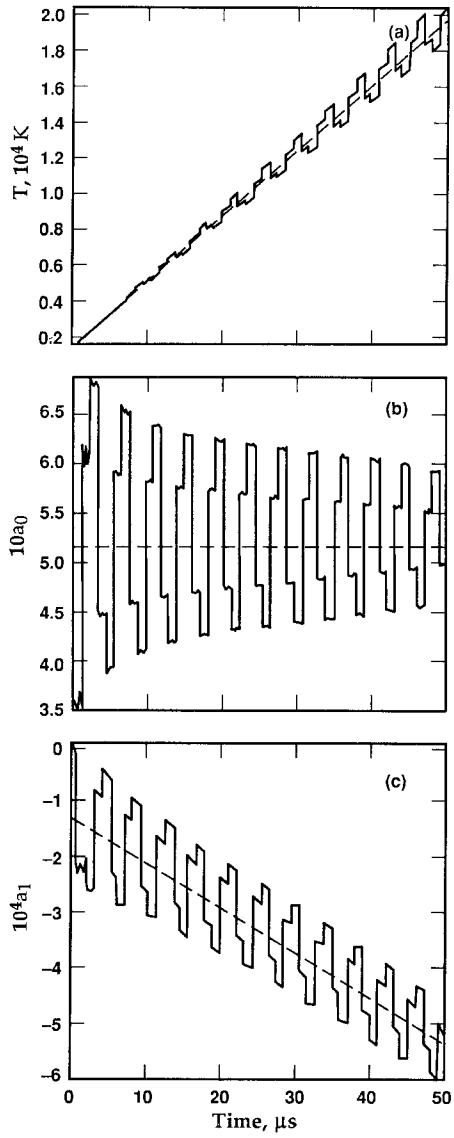

Fig. 3. Measurement errors for T, a_0, and a_1 for problem 3, with Gaussian channels with 100-nm FWHM, 0.2% errors, and wavelengths 550, 650, and 750 nm.

channels with wide separation. Comparison of Figs. 2 and 3 shows that there is little dependence on the width of the channels used. One can thus use either relatively wide channels to gain sensitivity or narrow channels to avoid possible line radiation which may be present.

Babelot and Hoch [2] made fits to the tungsten emissivity data of DeVos [3], Larrabee [4], and Latyev et al. [5]. They considered three fit forms for the emissivity dependence. The one of interest here is the one with linear wavelength dependence:

$$\varepsilon(\lambda, t) = a_0(T) + a_1(T)\,\lambda \tag{16}$$

$$a_0(T) = b_0 + b_1 T \tag{17}$$

$$a_1(T) = c_0 + c_1 T \tag{18}$$

The fit to DeVos' [3] data is given by

$$\begin{aligned} b_0 &= 0.6166 & c_0 &= -2.199 \times 10^{-4} \\ b_1 &= -4.55 \times 10^{-5} & c_1 &= 3.88 \times 10^{-4} \end{aligned} \tag{19}$$

The fit to Larrabee's [4] data is

$$\begin{aligned} b_0 &= 0.5200 & c_0 &= -8.60 \times 10^{-5} \\ b_1 &= 0 & c_1 &= -3.25 \times 10^{-8} \end{aligned} \tag{20}$$

and the fit to the data of Latyev et al. [5] is

$$\begin{aligned} b_0 &= 0.6236 & c_0 &= 2.312 \times 10^{-4} \\ b_1 &= -5.31 \times 10^{-5} & c_1 &= 4.49 \times 10^{-8} \end{aligned} \tag{21}$$

Three additional problems were run using the emissivity fits for each source of data, to examine how much results are influenced by target characteristics. Gaussian channels with 50-nm FWHM, wavelengths 500, 700, and 900 nm, and 0.2% errors were assumed. Since the fits to the data of DeVos [3] and of Latyev et al. [5] could not be extrapolated to as high a temperaure as the fit to Larrabee's [4] data without giving unphysical results, comparisons were made to a maximum temperature of 11000 K. It was found that the measurement errors at the highest temperatures are least for the Larrabee [4] emissivity. For the data of DeVos [3] and of Latyev et al. [5], the decrease in emissivity with temperature causes the predicted detector outputs to eventually decrease at the higher temperatures. The measurement errors are indeed influenced by the emissivity characteristics of the target. It should be pointed out that this is not

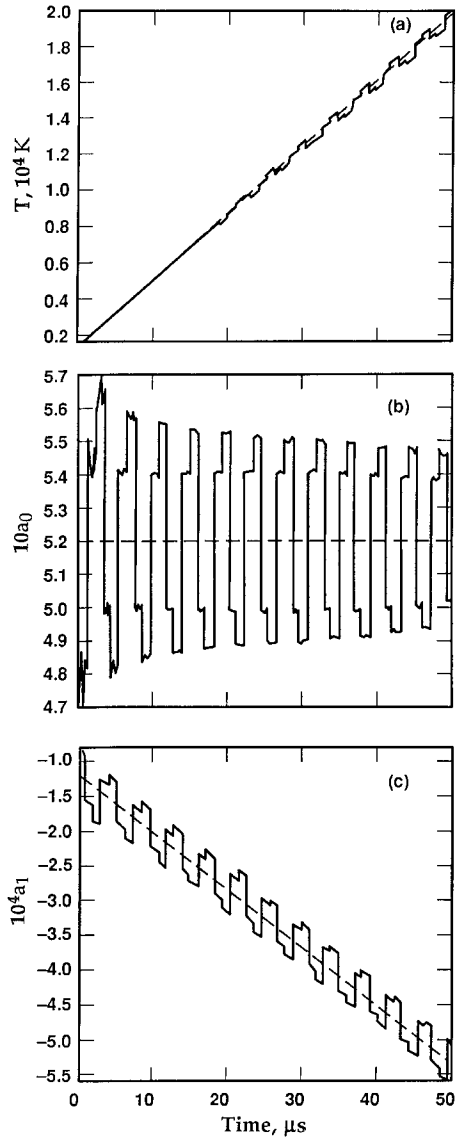

Fig. 4. Measurement errors for T, a_0, and a_1 for problem 4, using the example pyrometer of [1] with Babelot and Hoch's [2] fit to Larrabee's [4] tungsten data, and 0.2% errors, without the fiber-optic light-pipe.

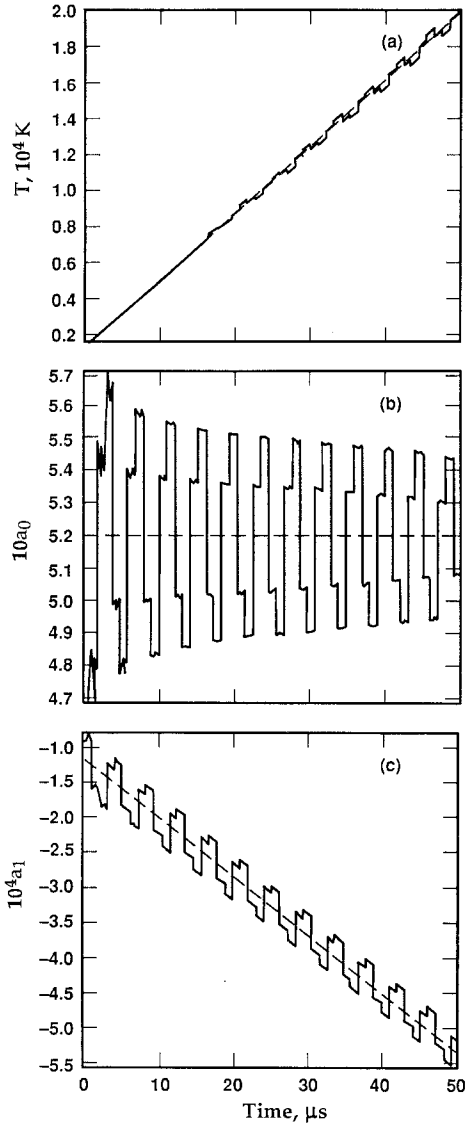

Fig. 5. Measurement errors for T, a_0, and a_1 for problem 5, using the example pyrometer of [1] with Babelot and Hoch's [2] fit to Larrabee's [4] tungsten data, and 0.2% errors, with the fiber-optic light-pipe attached.

systematic error, since the data were generated using the same model as that used in the data reduction.

A final set of two problems was run using the example pyrometer described in the preceding paper [1]. Since the fit to Larrabee's [4] data can be extrapolated to higher temperatures, it was chosen to represent an assumed tungsten target. Problem 4 corresponds to the bare pyrometer, without fiber-optic light-pipe. Problem 5 corresponds to the pyrometer with light-pipe attached. Figures 4 and 5 show the corresponding results. Comparison of the two figures shows that for this pyrometry scheme, the fiber-optic light pipe has little influence.

A Monte Carlo analysis was made to compare with the predictions of the modulation method. The example pyrometer with the fiber-optic light-pipe attached was used with Babelot and Hoch's [2] fit to Larrabee's [4] tungsten emissivity data. Simulated data were generated as before, and randomly distributed errors of 0.2% of the signal level were added to the data. A series of 10 runs was made using a randomly chosen seed for each run. At each time point a series of 10 sets of temperature and emissivity coefficient values was thus produced and was used to calculate the mean and standard deviation for each parameter.

The resulting curves for the standard deviation versus temperature were smoothed by least-squares fitting and are shown in Fig. 6. The solu-

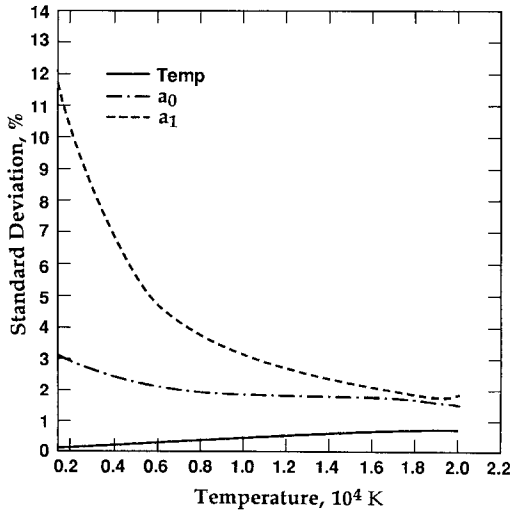

Fig. 6. Standard deviation for T, a_0, and a_1 as a function of true temperature, obtained with Monte Carlo methods. The standard deviation for each successive variable solved for increases because of error propagation.

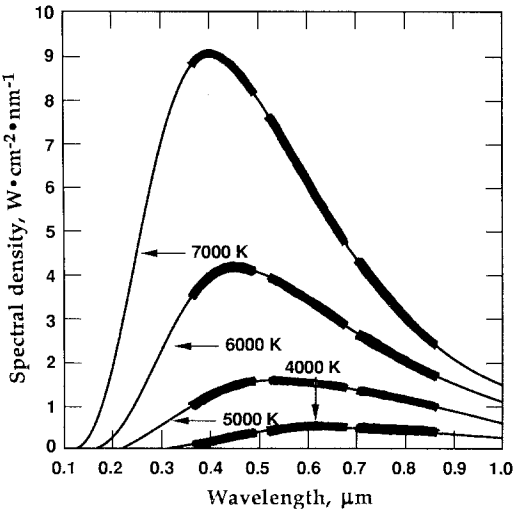

Fig. 7. Spectral placement of the channels of the example pyrometer with fiber-optic light-pipe in [1] for a series of temperatures using Babelot and Hoch's [2] fit to Larrabee's [4] tungsten emissivity data.

tion sequence for the parameters is T, a_0, and a_1, and as a result of error propagation, the standard deviation for each successive parameter becomes larger. For the temperature, the standard deviation grows to about 0.8% at 20,000 K. The standard deviation of the emissivity parameters generally drops as the temperature increases. This can be seen to be consistent with the predictions of the modulation method, as seen in Fig. 5, corresponding to the same pyrometer and emissivity model (for Larrabee's [4] emissivity, the parameter a_0 is constant). At a temperature of about 18,000 K, the temperature deviation is about 3.5 standard deviations, while for a_0 and a_1 the deviation is about 2.7 and 3.2 standard deviations, respectively.

Table I. Percentage Deviation in Calculated Temperatures and Emissivity Coefficients at Temperatures of Approximately 4650 K and 18,600 K for Input Data Errors of 0.2%

Problem No.	T		a_0		a_1	
	4650 K	18,600 K	4650 K	18,600 K	4650 K	18,600 K
1	0.78	1.83	−6.08	−3.44	−13.3	−3.58
2	2.85	7.50	−21.3	−13.5	−49.0	−14.5
3	2.86	7.23	−21.5	−13.2	−49.5	−14.4
4	0.71	2.14	−7.69	−4.84	−17.7	−5.56
5	0.73	2.17	−6.89	−4.83	−17.7	−5.47

Figure 7 shows the spectral placement of the channels for the example pyrometer with the light-pipe attached, for a series of temperatures, using Babelot and Hoch's [2] fit to the tungsten emissivity of Larrabee [4]. Above a few thousand degrees, the channels move to the red side of the spectral maximum. Figure 6 shows that for the three-color scheme, unlike ratio pyrometry, the shift to the red side of the spectrum has no severe consequences.

4. CONCLUSIONS

The modulation method for evaluating the sensitivity of a pyrometer to measurement errors can be used to evaluate proposed pyrometry schemes. For the particular example given, the results show that the relative errors in the calculated temperature are significantly larger than those of the input data. Comparison of Fig. 4b in the preceding paper [1] with problem 1 in Table I indicates that the three-color scheme gives comparable or possibly worse results. The results for the ratio pyrometer are the worst-case bounds, while the measurement errors for the three-color method could be even greater than calculated. The errors in the emissivity coefficients are so large that the derived values are of little practical use. As with the case of ratio pyrometry, it is seen that wide wavelength placement of the channels is advantageous, but channel width has little influence. These conclusions are consistent with those of Coates [6], Nordine [7], Gardner [8], and Snopko [9].

ACKNOWLEDGMENT

This work was performed under the auspices of the U.S. Department of Energy by the Lawrence Livermore National Laboratory under Contract W-7405-ENG-48.

REFERENCES

1. G. R. Gathers, *Int. J. Thermophys.* **13**:173 (1992).
2. J. F. Babelot and M. Hoch, *High Temp. High Press.* **21**:79 (1989).
3. J. C. DeVos, *Physica* **20**:690 (1954).
4. R. D. Larrabee, *J. Opt. Soc. Am.* **49**:619 (1959).
5. L. N. Latyev, V. Ya Chekhovskoi, and E. N. Shestakov, *High Temp. High Press.* **2**:175 (1970).
6. P. B. Coates, *High Temp. High Press.* **20**:433 (1988).
7. P. C. Nordine, *High Temp. Sci.* **21**:97 (1986).
8. J. L. Gardner, *High Temp. High Press.* **12**:699 (1980).
9. V. N. Snopko, *High Temp. High Press.* **25**:724 (1987).